

# Pseudo-Dynamic Active Earth Pressure Analysis of Inclined Retaining Walls Using Horizontal Slices Method

A. Ghanbari<sup>1,\*</sup> and M. Ahmadabadi<sup>1</sup>

**Abstract.** Retaining walls may be constructed with an inclination angle of less than  $90^\circ$  from the horizontal axis. In the present study, using the horizontal slices method and limit equilibrium principles, in addition to assuming variation of the seismic coefficient with height, a new formulation is proposed to calculate the active seismic pressure on retaining walls. The general arrangement of the proposed pseudo-dynamic formulation allows analysis of inclined or vertical retaining walls in frictional, cohesive and cohesive-frictional soils. Results from the proposed method were compared with those of previous researchers under similar conditions and showed a negligible difference. The horizontal slices method was able to assess an inclined wall, determine the active earth pressure distribution at different points along the wall height and consider the angle of failure wedge as a variable in the time domain. The findings show that despite the accepted assumptions for conventional vertical walls the distribution of earth pressure on an inclined wall follows a non-linear pattern at each moment.

**Keywords:** Inclined retaining wall; Horizontal slices method; Pseudo-dynamic; Active earth pressure.

## INTRODUCTION

Retaining walls are designed to withstand stresses caused by lateral earth pressure. The magnitude of this pressure is a function of the soil properties, the wall and the intensity of static and dynamic loads. The inclination of a wall plays a major role in the reduction or increase in lateral earth pressure. An increase in the inclination angle from the vertical state decreases lateral earth pressure. Theories to calculate static and seismic pressures on retaining walls are usually only for vertical conditions; applied pressure on inclined retaining walls has rarely been a matter of concern. Figure 1 is an example of walls analyzed by previous researchers where the wall does not incline toward the soil mass, as opposed to the inclined retaining wall, which is the subject of the present study.

Inclined walls are subjected to less lateral earth pressure than vertical walls, even to the point where at times the static earth pressure on an inclined wall becomes zero. Inclined walls are employed in

1. Faculty of Engineering, Tarbiat Moallem University, Tehran, P.O. Box 15614, Iran.

\*. Corresponding author. E-mail: ghanbari@tmu.ac.ir

Received 7 June 2009; received in revised form 10 December 2009; accepted 18 January 2010

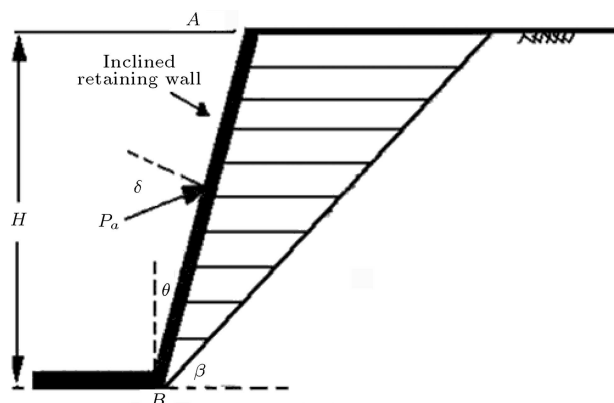


**Figure 1.** Deviation of failure wedge into horizontal slices for an inclined retaining wall.

embankment dams as lateral spillway walls, in coastal structures, such as quay walls and in road building projects as road protectors and on sideways slopes.

This paper first reviews theories of previous researchers and then proposes, using the horizontal slices method, to calculate seismic pressure on inclined walls. In the proposed method, a variation of input-triggering acceleration with time is considered and a pseudo-dynamic analytical solution is proposed for retaining walls for the common range of periods.

Recent studies of geotechnical structures include experimental studies, numerical analysis and analytical models. Analytical models include the homogenized analytical concept, limit analysis, limit equilibrium, the horizontal slices method and the characteristics method [1-8].

Measuring earth pressure on retaining structures for granular soils in static conditions has usually been performed using Rankine's [9] or Coulomb's [10] methods. However, Caquot and Kerisel [11], Sokolovskii [12], Lee and Herrington [13] and Hua and Shen [14] have all advanced significant procedures to estimate static lateral earth pressure in granular soils.

To calculate seismic pressure, one of the oldest theories proposed was by Okabe [15] and Mononobe and Matsuo (M-O) [16]. This technique has been presented using Coulomb's theory [10] and assuming the pseudo-static method to be valid for granular soils. In the M-O method, equilibrium relations are formulated for a rigid wedge, assuming the seismic coefficient to be constant along the wall, and ignoring soil cohesion seismic pressure on the wall is achieved. This method assumes stress distribution of the soil on the wall to be linear.

The influence of phase on the calculation of pseudo-static earth pressure on a retaining wall and behavior of quay walls in earthquakes was investigated by Steedman and Zeng [17], Zeng and Steedman [18], Chang [19] and Choudhury et al. [5]. Cheng [19] suggested the rotation of axes as a solution for slip line equations to determine lateral earth pressure under general conditions. Chang [19] also proposed a method based on pseudo-static analysis assumptions that contain all the limitations of the M-O method.

Recently, researchers have calculated pressure applied to retaining walls using pseudo-static and pseudo-dynamic analysis. Choudhury and Nimbalkar [20,21] as well as Shekarian et al. [22] calculated the seismic pressure on retaining walls using a limit equilibrium technique. These studies were formulated for vertical walls with cohesionless backfill and under pseudo-static conditions to address seismic acceleration. Nimbalkar et al. [23], Nimbalkar and Choudhury [6], Ahmad and Choudhury [24], Shekarian and Ghanbari [25] and Azad et al. [26] also studied seismic pressure under pseudo-dynamic conditions for vertical walls in granular soils. Finally, Ghosh [27] considered a method to calculate the seismic pressure and angle of failure wedge for inclined walls with linear variations of acceleration by height.

The present study used the horizontal slices method and assumed pseudo-dynamic analysis to determine seismic stress distribution on retaining walls, the angle of failure wedge and the application point of the resultant force. The proposed method eliminates the limitations of previous techniques and ascertains

seismic pressure for an inclined wall with cohesive-frictional backfill. Moreover, this method is able to determine the non-linear stress distribution at different depths of an inclined wall.

## HORIZONTAL SLICES METHOD

Originally, slices, especially in the conventional vertical slices method, were used to estimate slope stability. Shahgholi et al. [28] introduced one method to determine such slopes. The Horizontal Slices Method (HSM) was expanded upon by Nouri et al. [8,29] by addressing the seismic acceleration at different heights of a structure. Azad et al. [26], Shekarian and Ghanbari [25], Shekarian et al. [22] and Ahmadabadi and Ghanbari [7] employed HSM within the framework of pseudo-dynamic and pseudo-static methods to ascertain seismic active earth pressure on retaining walls. HSM is able to determine the distribution of seismic active earth pressure and the application point of the resultant earth pressure.

To determine the active earth pressure of a retaining wall with reinforced and unreinforced cohesive-frictional backfill using HSM, the following assumptions were made in the present study:

1. The application point of the vertical inter-slice force is located at the surface-center of the stress distribution curve derived from the succeeding equations.
2. The failure surface is planar.
3. The method is limited to homogeneous masses.
4. The failure surface is assumed to pass through the heel of the wall.
5. The value of the shear force between horizontal slices is unequal ( $H_i \neq H_{i-1}$ ).
6. The point where  $N_i$  acts on the slice base is located at the midpoint of that base.
7. The point where  $P_i$  acts is located at mid-height for each slice.

## PROPOSED METHOD

An arbitrary wall with height  $H$  and inclination slope  $\theta$  is shown in Figure 1, representing a general method for seismic pressure calculations on retaining walls. The interface of failure wedge and backfill soil forms angle  $\beta$  with the horizontal axis. The failure wedge is divided into  $n$  slices with equal thicknesses of  $h_i = \frac{H}{n}$ . The applied forces on the  $i$ th slice are shown in Figure 2. Distances in Figure 2 can be calculated using the

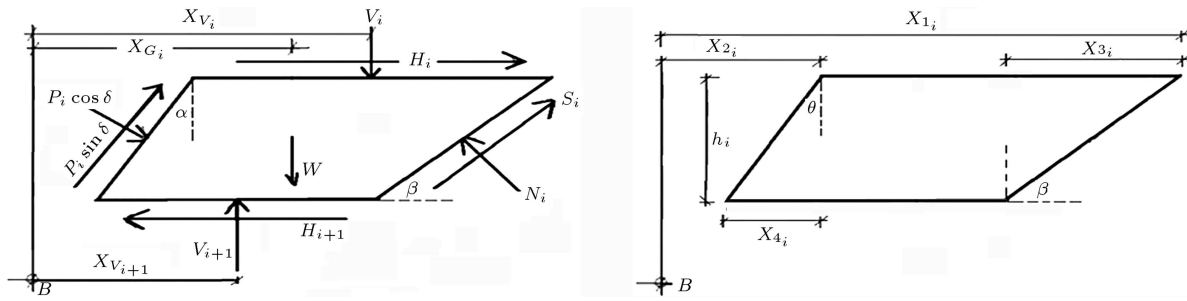


Figure 2. Equilibrium of forces on the  $i$ th slice.

following equations:

$$X1_i = \frac{\sum_{j=1}^n h_j}{\tan(B)}, \quad (1)$$

$$X2_i = \left[ \sum_{j=i}^n h_j \right] \tan(\theta), \quad (2)$$

$$X1_{i+1} = \frac{\sum_{j=i+1}^n h_j}{\tan(\beta)}, \quad (3)$$

$$X3_i = \frac{h(i)}{\tan \beta}, \quad (4)$$

$$X4_i = h(i) \tan \theta, \quad (5)$$

$$X_{G_i} = \frac{x1_i}{2} + \frac{x2_i}{2} - \frac{x3_i}{4} - \frac{x4_i}{4}. \quad (6)$$

The weight of each slice can be determined as:

$$W_i = \gamma_i \left\{ (x1_i - x2_i - x3_i)h_i + \frac{(x4_i + x3_i)}{2}h_i \right\}. \quad (7)$$

To calculate the vertical stress acting between slices, the equation suggested by Segrestin [30] was employed in which the variations of vertical stress for each horizontal plane are addressed as:

$$v_i = \gamma z_i \cdot \eta. \quad (8)$$

In the above equation,  $Z$  is the depth of the horizontal plane from the top of the wall and  $\eta$  is a coefficient smaller than unity and calculated by a tangent-hyperbolic function for all points in the horizontal plane. Shekarian et al. [22] have described this calculation in detail. Notice that the application of this equation increases the precision of the analysis for inclined walls in comparison with the findings of researchers who estimated the value of vertical stress as:

$$v_i = \gamma z_i.$$

The horizontal and vertical seismic forces on each slice are  $F_h$  and  $F_v$ , respectively, which can be determined as a fraction of the weight of the sliding wedge:

$$F_{h_i} = a_h(z, t) \cdot w_i, \quad (9)$$

$$F_{v_i} = a_v(z, t) \cdot w_i. \quad (10)$$

Seismic active earth pressure can be obtained similar to Steedman and Zeng [17] and Choudhury and Nimbalkar [20] using the pseudo-dynamic method for backfill soil. In the proposed method, it is assumed that the base of the inclined wall is subject to both horizontal and vertical harmonic vibrations with amplitudes of accelerations of  $a_h (= k_h g)$  and  $a_v (= k_v g)$ , respectively, which begin at exactly the same time and with no phase shift between them, thus, providing critical design criteria. Variations of  $\alpha_h(z, t)$  and  $\alpha_v(z, t)$  are considered as sine functions in:

$$a_h(z, t) = K_h g \left( \sin \omega \left( t - \frac{H - z}{v_s} \right) \right), \quad (11)$$

$$a_v(z, t) = K_v g \left( \sin \omega \left( t - \frac{H - z}{v_p} \right) \right), \quad (12)$$

where  $t$  is time,  $V_s$  and  $V_p$  are velocity of shear and pressure waves in the soil, respectively, and  $K_h$  and  $K_v$  are the amplitudes of seismic acceleration coefficients in the horizontal and vertical directions, respectively. For most geotechnical materials, accepting the relation  $\frac{V_p}{V_s} = 1.87$  is appropriate [31]. In the pseudo-static condition, variations of horizontal and vertical coefficients with time are assumed to be constant. However, time has an effect in the pseudo-dynamic condition, thus, causing horizontal and vertical coefficient accelerations to differ depending on the period considered for the seismic load. Variations of the horizontal acceleration coefficient along the height of a wall for the two conditions  $T = 0.2$  and  $T = 0.8$  are illustrated in Figure 3. As can be observed, at the moment of  $t$  and for each period of  $T$ , the seismic acceleration coefficient had a non-linear distribution along the wall.

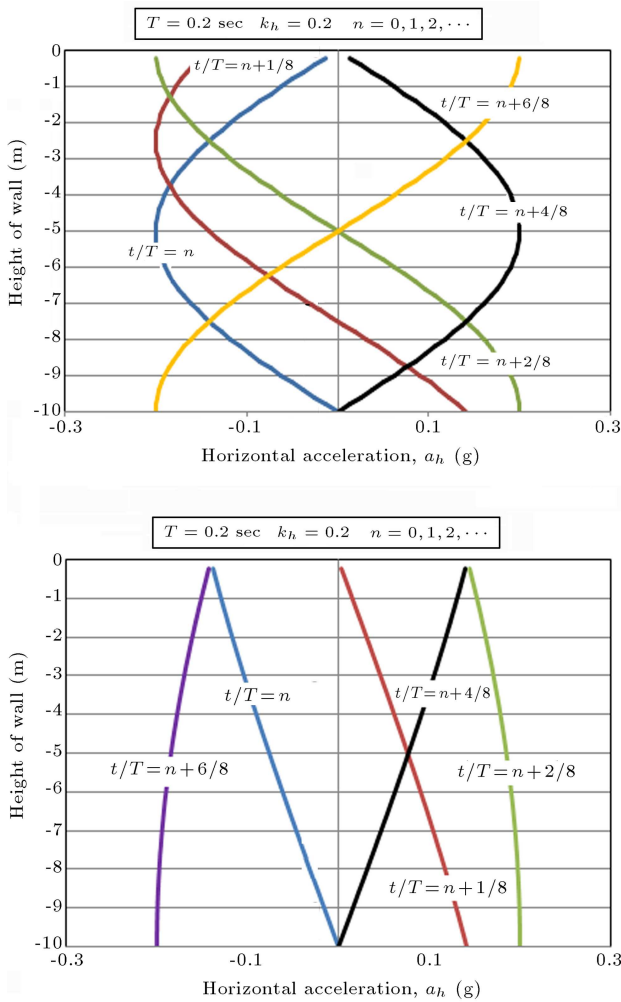


**Figure 3.** Variations of horizontal pseudo-dynamic acceleration along the height of the wall for  $T = 0.2, 0.8$  sec.

Based on these assumptions, three equations for the equilibrium of forces and moments and one for the shear strength of soil were formulated for each moment and each horizontal slice. The applied pressure on each slice at different points on a wall at each moment can be determined by solving the equation set with  $4n$  unknowns and  $4n$  equations:

$$\begin{aligned} \sum F_x(t) = 0 \longrightarrow & H_i(t) - H_{i+1}(t) - F_{h_i}(t) \\ & + S_i(t) \cos \beta(t) - N_i(t) \sin \beta(t) \\ & + P_i(t) \cos \delta \cos \theta + P_i(t) \sin \delta \sin \theta = 0, \quad (13) \end{aligned}$$

$$\begin{aligned} \sum F_y(t) = 0 \longrightarrow & -V_i(t) + V_{i+1}(t) + F_{v_i}(t) - W_i(t) \\ & + S_i(t) \sin \beta(t) + N_i(t) \cos \beta(t) \\ & - P_i(t) \cos \delta \sin \theta + P_i(t) \sin \delta \cos \theta = 0, \quad (14) \end{aligned}$$

$$\begin{aligned} \sum M_o(t) = 0 \longrightarrow & -V_i(t)X_{V_i} + V_{i+1}(t)X_{V_{i+1}} \\ & + (F_{h_i}(t) - W(t)_i)X_{G_i} \\ & + \left[ F_{h_i}(t) + \frac{N_i(t)}{\sin \beta_i(t)} - \frac{P_i(t) \cos \delta}{\cos \theta} \right] \\ & \times \left[ \sum_{j=i+1}^n h_j + \frac{h_i}{2} \right] + H_{i+1}(t) \sum_{j=i+1}^n h_j \\ & - H_i(t) \sum_{j=i}^n h_j = 0, \quad (15) \end{aligned}$$

$$S_i(t) = [N_i(t) \tan \phi + c\{h_i / \sin(\beta)\}]. \quad (16)$$

Knowing the force of each slice, the non-linear pressure distribution applied to the wall can be determined and the resultant force calculated:

$$P(t) = \sum_{i=1}^n P_i(t). \quad (17)$$

The value of the angle of failure wedge ( $\beta$ ) depends on the applied stresses on the soil mass at each moment. To calculate  $\beta$ , the maximum active pressure on the wall is applied by the failure wedge and is written as:

$$\frac{\partial P_i(t)}{\partial \beta} = 0. \quad (18)$$

The equations and unknowns of the formulation are summarized in Table 1.

## RESULTS

The proposed formulation can calculate the active pressure on the wall for each moment as well as for the angle of failure wedge. To this end, the model inclined wall illustrated in Figure 4 was analyzed under a sine harmonic seismic load with period  $T$ . The properties of this wall are noted in Table 2.

Variations in the pressure and angle of the failure wedge over time were studied for the vertical retaining wall with granular backfill. Since the pressure applied to the wall is determined by limit equilibrium, it represents the active state for the soil and is indicated by  $Pa(t)$ . This pressure is a combination of the active static pressure and the excess dynamic pressure due to seismic loading. Figure 5 shows the variations in the active earth pressure and angle of failure wedge in the first second of loading for the model wall for a period of 0.2 sec. The magnitude of this pressure is related to the slope of the internal face of the wall. It is proposed that the slope of the axis of the wall is equal to the slope of the internal face of the wall. The slope

**Table 1.** Equations and unknowns for horizontal slices method in the pseudo-dynamic state.

Unknowns	Number	Equations	Number
$H_i(t)$	$n$	$\sum F_x(t) = 0$	$n$
$N_i(t)$	$n$	$\sum F_y(t) = 0$	$n$
$S_i(t)$	$n$	$\sum M_0(t) = 0$	$n$
$P_i(t)$	$n$	$S_i(t) = [N_i(t) \tan \phi + c\{h_i / \sin(\beta(t))\}]$	$n$
_____	$4n$	_____	$4n$

**Table 2.** Properties of the model wall for pseudo-dynamic analysis.

Series	Height of Wall ( $H$ ) (m)	Cohesion of Soil ( $c$ ) (kN/m <sup>2</sup> )	Internal Friction Angle ( $\phi$ ) (degrees)	Specific Weight of Soil ( $\gamma$ ) (kN/m <sup>3</sup> )	Friction Angle Between Soil and Wall ( $\delta$ ) (degrees)	Inclination Angle of Wall ( $\theta$ ) (degrees)	Horizontal Seismic Coefficient ( $K_h$ )
1	10.0	0.0	30	20.0	$2\phi/3$	0.0	0.2
2	10.0	20.0	30	20.0	$2\phi/3$	0.0	0.2
3	10.0	0.0	30	20.0	$2\phi/3$	0.0 – 30.0	0.1 – 0.4
4	10.0	0.0 – 20.0	30 – 40	20.0	$2\phi/3$	0.0 – 30.0	0.0 – 0.2

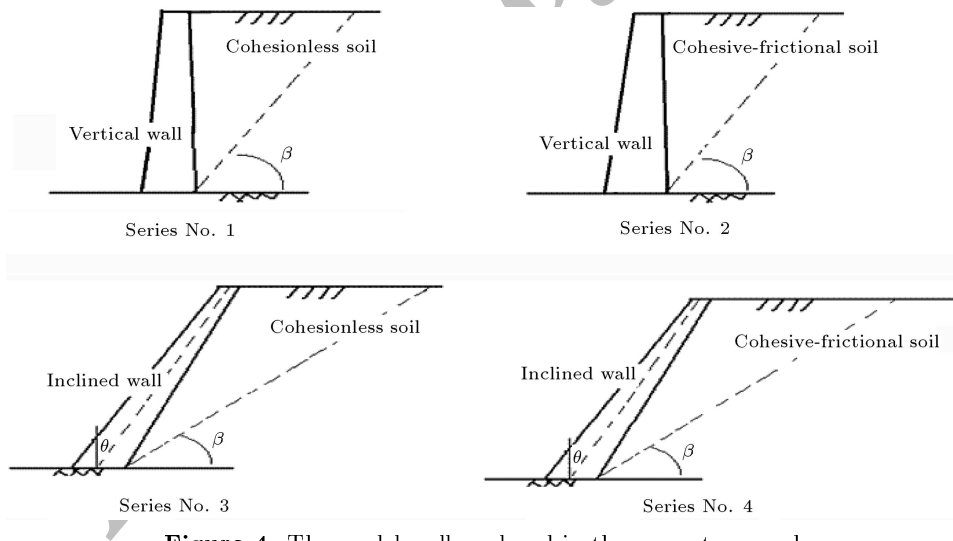


**Figure 4.** The model wall analyzed in the present research.

of the outer face of the wall only changes the axis of the wall and has no effect on the active earth pressure magnitude.

Figure 6 illustrates the variations of active pressure ratio versus time for the range of periods between 0.2 and 1.0 sec. The maximum pressure ratio on the wall occurred between 0.1 to 0.3 sec from the beginning of loading and its value was between 0.4 and 0.45. Figure 7 shows the angle of failure wedge during the pseudo-dynamic loading at different periods. The angle of failure wedge was between 43° and 62° and decreased

as the minimum period increased. The applied seismic load is a sine harmonic load with a period of  $T$  and its direction changes continuously. When the direction of the seismic load is left to right, the active earth pressure decreased. In this state, the behavior of the soil changed from active to passive and the angle of failure wedge decreased.

The second stage of analysis was performed on a vertical wall with cohesive-fictional backfill. Figure 8 shows the variations in active earth pressure and the angle of failure wedge for 0.2 and 0.4 sec compared with

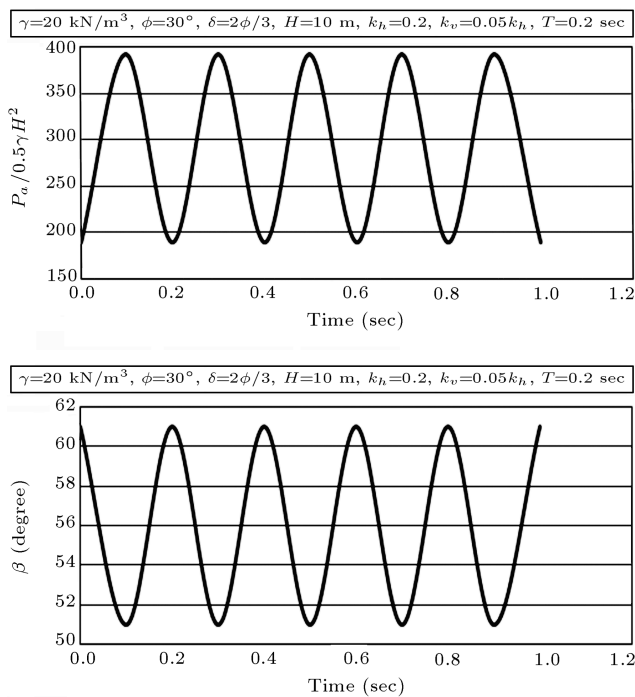


**Figure 5.** Variation of pressure applied to the wall and angle of failure wedge for a unit of time.

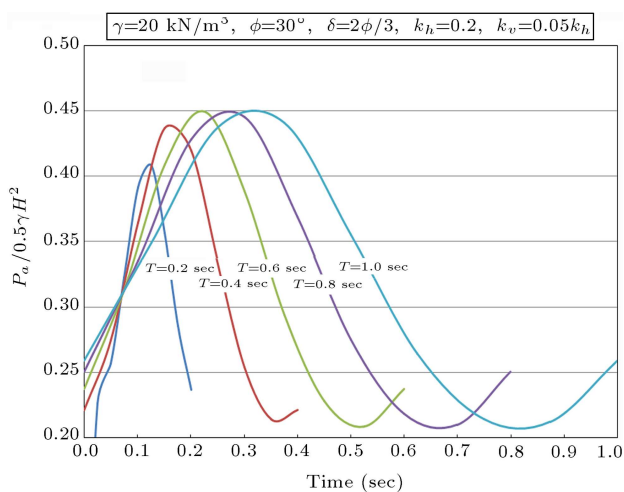


**Figure 6.** Variations of applied force to the wall versus time for different periods.

the results for non-cohesive soil. As can be observed, active earth pressure on the wall with cohesive backfill for a specific time was similar to granular soil, yet is of lower value. Also, the angle of failure wedge in cohesive soil was larger than that for frictional soil and this difference was approximately the same for each period.

The third analysis was performed for an inclined wall with granular backfill. The seismic pressure distribution for an inclined wall in a static state is shown in Figure 9. As can be seen, earth pressure distribution on the wall is non-linear and, thus, the

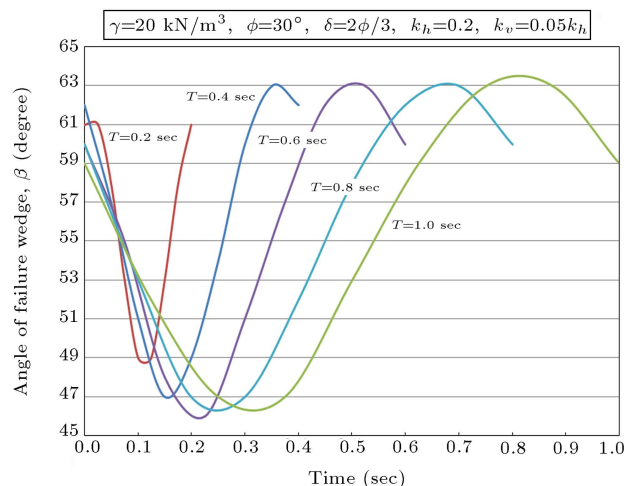


**Figure 7.** Angle of critical failure wedge versus time for different periods.

application point of the static resultant force is at a distance of less than one-third the height of the wall. Choudhury and Nimbalkar [21] and Ghosh [27] have reported non-linear pressure distribution behind the wall. However, in most previous studies, this was ignored because it was assumed that the pressure applied to the wall was linear. In the present study, since the backfill was divided into several horizontal slices, the stress distribution was accurately determined and it was shown that this distribution is non-linear for inclined walls.

The application point of the force in the pseudo-dynamic state ( $Z_c(t)$ ), assuming the equality of the two acting moments, the resultant force and applied pressure moments, can be determined as follows:

$$\sum_{i=1}^n \left\{ P_i(t) \cos(\delta + \theta) \times \left[ \sum_{j=i}^n h_j + \frac{h_i}{2} \right] \right\} = P_a(t) \cos(\delta + \theta) \times Z_c(t), \quad (19)$$

$$Z_c(t) = \frac{\sum_{i=1}^n \left\{ P_i(t) \times \left[ \sum_{j=i}^n h_j + \frac{h_i}{2} \right] \right\}}{p_a}. \quad (20)$$

The ratio of the height at which the pseudo-dynamic force acts on the height of the wall is shown for different periods in Figure 10. These results show that the maximum ratio was about 0.35, the same for all periods for the model wall. The results of the third stage analysis for an inclined wall in granular soil are shown in Figure 11, in comparison with similar values for a vertical wall.

Variations in the angle of failure wedge versus angle of internal friction are depicted in Figure 12 for an inclined wall for different seismic load domains.

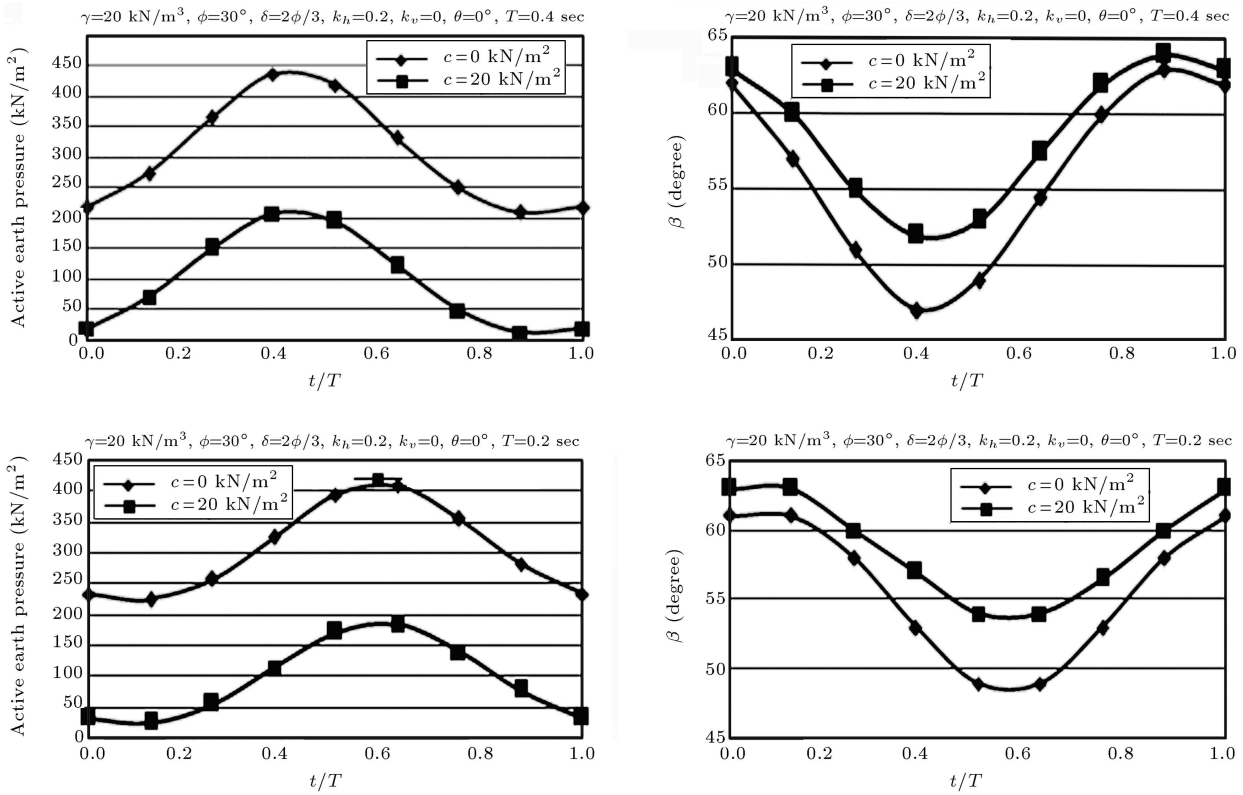


Figure 8. Change in active earth pressure and angle of failure wedge in cohesive-frictional soils.

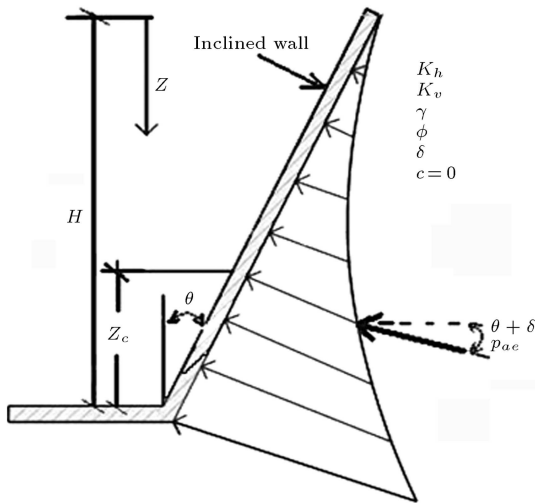


Figure 9. Stress distribution in the presence of a seismic load.

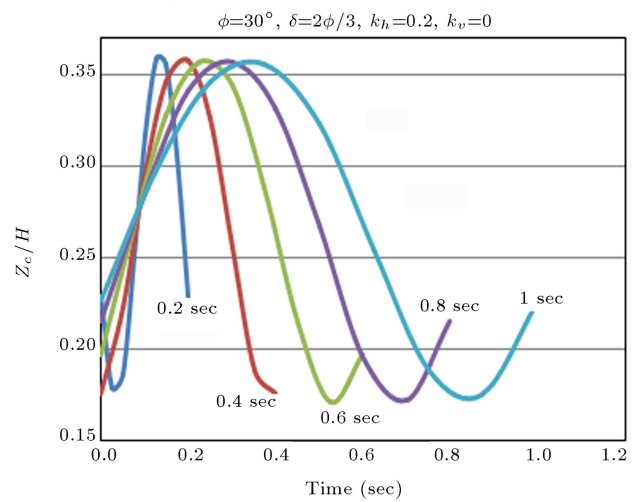


Figure 10. Change in the application point of resultant force versus time for different periods.

Variations of these angles by the inclination angle of the wall are shown in Figure 13. It can be observed in these figures that with an increase in the inclination of the wall and a decrease in the angle of internal friction, the angle of failure wedge decreased.

The fourth stage of analysis focused on an inclined wall with cohesive-frictional backfill, the most complete case for pseudo-static analysis where the limitations of previous methods are absent. Figure 14 shows the raw

active pressure distribution of the cohesive-frictional backfill on an inclined wall for slopes varying from zero to 20°. An increase in the slope of the wall reduced the pressure applied to the wall, however, the distribution was non-linear for all conditions. Variations of active pressure against the friction angle of the soil are shown in Figure 15.

The results show that when the friction angle of soil in the model wall was 40°, the applied pressure to

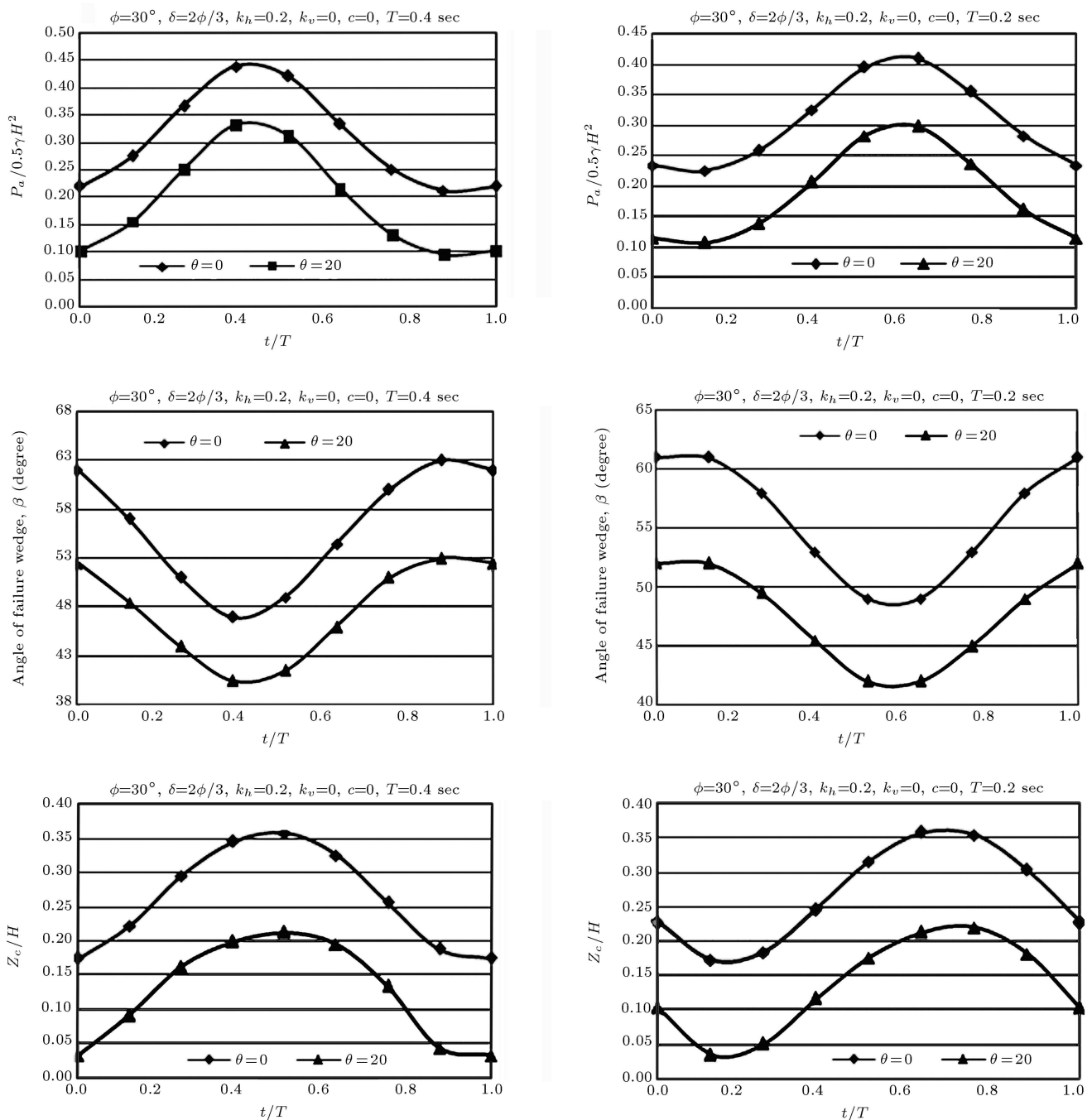


Figure 11. Analysis results for the third series for an inclined wall with granular backfill.

the wall was negative and no pressure was generated by the soil on the wall. This result is more accurate than results obtained from previous methods in which pressure distribution was assumed to be linear and, accordingly, the depth of the tensile cracks calculated by the proposed method differs from those of other methods.

Figure 16 shows the effect of the seismic load domain ( $K_h$ ) on the pressure applied to the wall by the cohesive-frictional backfill. It is shown that, with an increase in the seismic load domain, pressure applied

to the wall increased, yet the non-linear distribution remained valid. Figure 17 shows the linear trend of the increase in the angle of failure wedge with an increase in the internal friction angle of the soil for an inclined wall with cohesive-frictional backfill for different cohesions.

### COMPARISON OF METHODS

Several methods can be used to calculate seismic active earth pressure on inclined walls, all of which



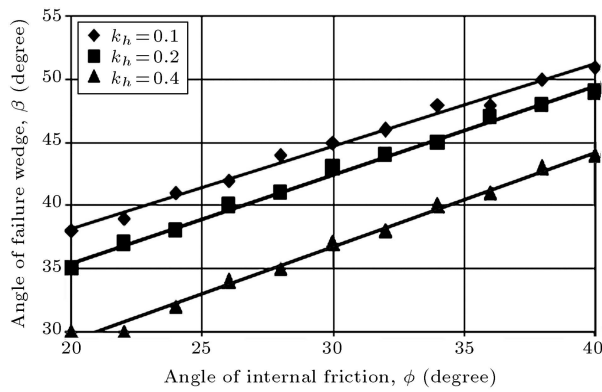


**Figure 12.** Change in the angle of failure wedge versus angle of internal friction for different horizontal seismic pressure coefficients  $c = 0 \text{ kN/m}^2$ ,  $\delta = 2\phi/3$ ,  $\theta = 20^\circ$ ,  $\alpha = 0$  and  $K_v = 0.5K_h$ .

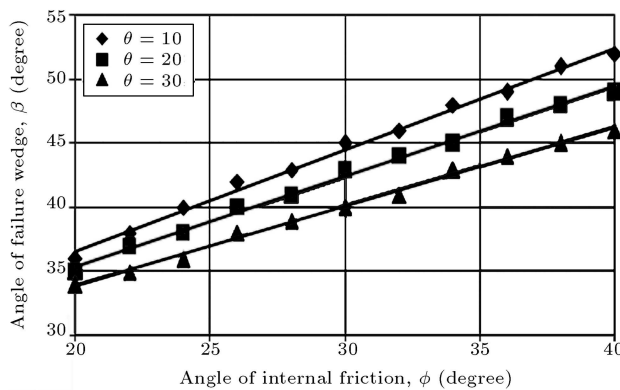


**Figure 13.** Change in the angle of failure wedge for different wall slopes  $K_h = 0.2$ ,  $\delta = 2\phi/3$ ,  $\alpha = 0$ ,  $c = 0 \text{ kN/m}^2$ ,  $K_v = 0.5K_h$ .

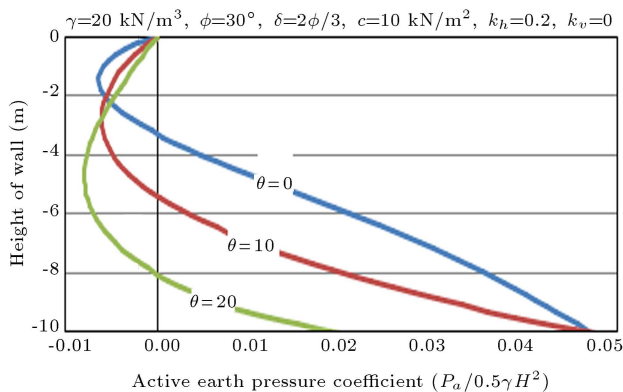


**Figure 14.** Pressure distribution versus active earth pressure for different slopes of an inclined wall.

present limitations and are limited to specific conditions. The current research uses limit equilibrium principles and assumes general conditions for the HSM method to analyze an inclined wall with cohesive-frictional backfill under pseudo-dynamic conditions. In this method, the seismic pressure coefficient of soil

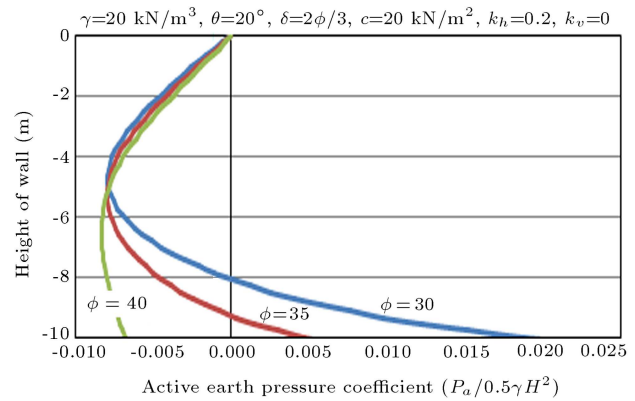


**Figure 15.** Stress distribution versus active earth pressure for different internal friction angles.

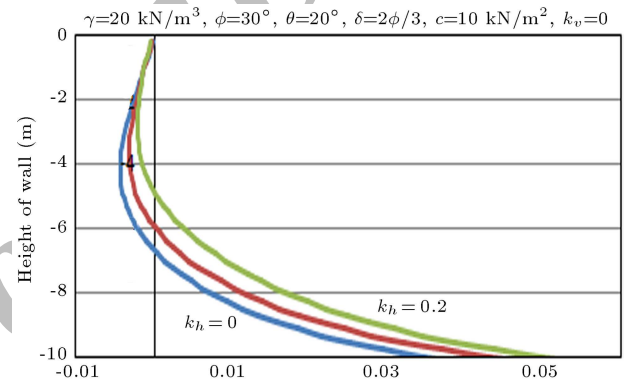


**Figure 16.** Stress distribution for different seismic pressure coefficients.

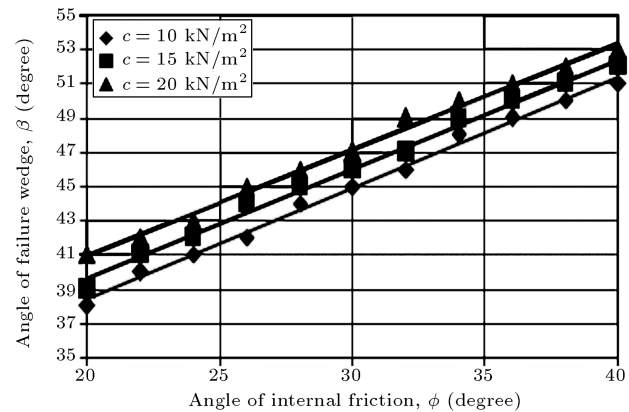


**Figure 17.** Change in the angle of failure wedge for different cohesions  $K_h = 0.2$ ,  $\delta = \phi/3$ ,  $\alpha = 0$ ,  $\theta = 20$  and  $K_v = 0.5K_h$ .

varies with time and along the wall. The results from this proposed method can be compared with those of previous researchers under similar conditions.

Figure 18 shows a comparison of the proposed method results for a vertical [b] wall with granular

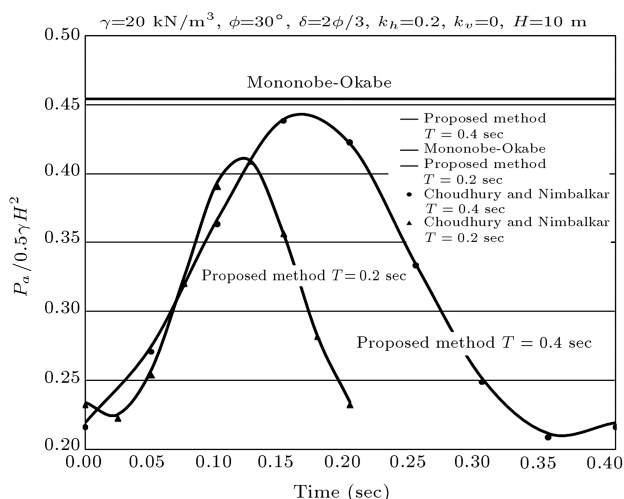


**Figure 18.** Comparison of applied seismic pressure to the wall for M-O and proposed methods.

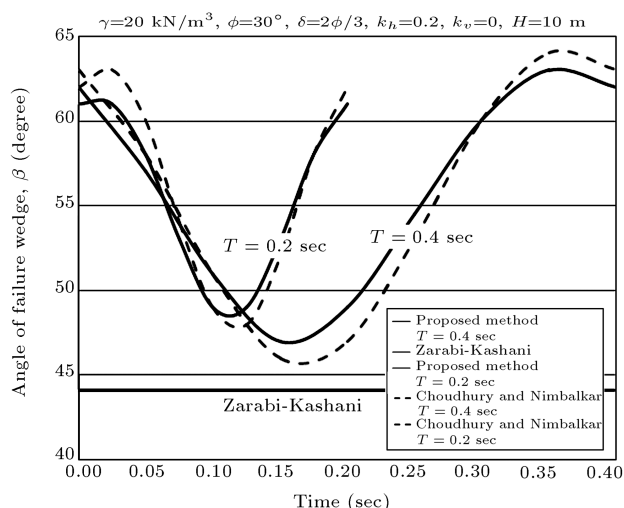


**Figure 19.** Comparison of seismic angle of failure wedge for Zarabi-Kashani and proposed methods.

backfill and results from the M-O method. The angle of failure wedge obtained from these methods is compared in Figure 19. The angle of failure wedge for the pseudo-static condition has been defined by Zarabi-Kashani [32] for the M-O method. As can be

observed, maximum seismic pressure in the proposed method varies between two limits and is a function of the load period. Figures 18 and 19 include similar results obtained by Choudhury and Nimbalkar [21] and Ghosh [27] using the pseudo-dynamic method and by Choudhury and Singh [33] using the pseudo-static method that highlight the merits of the pseudo-dynamic method.

The results for a vertical wall with granular backfill with active earth pressure to the wall and angle of failure wedge are compared to Choudhury and Nimbalkar [21] in Tables 3 and 4. Table 5 gives the results for a vertical wall under pseudo-dynamic conditions compared to Azad et al. [26]. Table 6 is a comparison of the results of the proposed method and Ghosh [27] for a vertical wall. In all cases, only minor differences were observed.

### CONCLUSION

A method was formulated using HSM for retaining walls under general conditions by which active earth pressure distribution on the wall and angle of failure wedge can be addressed in pseudo-dynamic conditions for seismic loads. This formulation, having  $4n$  equations and  $4n$  unknowns, was applicable for both vertical and inclined walls with cohesive, frictional and cohesive-frictional backfills.

The results showed that active pressure distribution for inclined walls was non-linear along the height of the wall, which differed from the linear distribution resulting from previous studies. Previous researchers considered the equilibrium of forces for the failure wedge, assuming a linear active pressure distribution along the wall. In the present study, the wedge was divided into several horizontal slices ( $\pm 1000$ ) and their equilibrium of forces and moments was calculated. It was concluded that the assumption of a linear earth pressure distribution for inclined walls differs significantly with actual cases. Therefore, the application point of the resultant force should be lower than those values reported by other researchers.

A comparison of the results with those of previous

**Table 3.** Comparison of active earth pressure coefficient for the proposed method and Choudhury and Nimbalkar's method [21].

$\alpha = 0^\circ, K_v = 0.5K_h, c = 0, \delta = \frac{2\phi}{3}, \theta = 0$						
	$K_h = 0.05$		$K_h = 0.1$		$K_h = 0.2$	
	Choudhury and Nimbalkar [21]	Proposed Method	Choudhury and Nimbalkar [21]	Proposed Method	Choudhury and Nimbalkar [21]	Proposed Method
$\phi = 20^\circ$	0.4539	0.4587	0.4674	0.4725	0.5020	0.5080
$\phi = 25^\circ$	0.3754	0.3793	0.3880	0.3923	0.4189	0.4239
$\phi = 30^\circ$	0.3108	0.3141	0.3226	0.3262	0.3510	0.3553

**Table 4.** Comparison of seismic angle of failure wedge (degrees) for the proposed method and Choudhury and Nimbalkar's method [21].

$\alpha = 0^\circ, K_v = 0.5K_h, c = 0, \delta = \frac{2}{3}\phi, \theta = 0$						
	$K_h = 0.05$		$K_h = 0.1$		$K_h = 0.2$	
	Choudhury and Nimbalkar [21]	Proposed Method	Choudhury and Nimbalkar [21]	Proposed Method	Choudhury and Nimbalkar [21]	Proposed Method
$\phi = 20^\circ$	48	48.1	46	46.0	41	41.2
$\phi = 25^\circ$	51	51.4	50	49.6	45	45.3
$\phi = 30^\circ$	55	54.5	53	53.0	49	49.4

**Table 5.** Comparison of results from proposed method and Azad et al.'s method [26].

$K_v = 0, K_h = 0.2, \delta = 0, \theta = 0, c = 0, \phi = 30^\circ, \gamma = 20 \text{ kN/m}^3, T = 0.2 \text{ sec}, V_s = 150 \text{ m/sec}$															
		$t = 0.0$		$t = 0.02$		$t = 0.04$		$t = 0.065$		$t = 0.08$		$t = 0.1$		$t = 0.12$	
		sec		sec		sec		sec		sec		sec		sec	
		$k_a$	$\beta$	$k_a$	$\beta$	$k_a$	$\beta$	$k_a$	$\beta$	$k_a$	$\beta$	$k_a$	$\beta$	$k_a$	$\beta$
$H = 3$ m	Proposed Method	0.29	62.5	0.358	58.2	0.431	54	0.470	51.8	0.449	53	0.384	57	0.311	61.8
	Azad et al. [26]	0.33	60.5	0.36	58	0.43	53	0.47	50	0.45	51	0.37	57	0.33	60
		$t = 0$		$t = 0.04$		$t = 0.06$		$t = 0.08$		$t = 0.12$		$t = 0.16$		$t = 0.2$	
		sec		sec		sec		sec		sec		sec		sec	
$H = 15$ m	Proposed Method	0.27	64.5	0.28	63	0.313	60.5	0.37	57	0.44	54	0.36	59.5	0.27	64.5
	Azad et al. [26]	0.33	60.5	0.34	59	0.355	58	0.38	56	0.48	52	0.39	57	0.33	60.5

$k_a$  = active earth pressure coefficient;  $\beta$  = angle of failure wedge (degrees).

**Table 6.** Comparison of results from proposed method and Ghosh's method [27].

$K_v = 0.5K_h, K_h = 0.2, \delta = 2\phi/3, c = 0, V_s = 100 \text{ m/sec}, V_p = 187 \text{ m/sec}, t = 0.47 \text{ sec}, T = 0.8 \text{ sec}$							
		$\theta = 0^\circ$		$\theta = 20^\circ$		$\theta = 30^\circ$	
		$\beta$	$k_a$	$\beta$	$k_a$	$\beta$	$k_a$
$\phi = 20^\circ$	Proposed Method	50.0	0.4440	41.0	0.2963	38.0	0.2482
	Ghosh [27]	50.0	0.4500	42.0	0.3270	38.0	0.2700
$\phi = 25^\circ$	Proposed Method	53.5	0.3637	44.5	0.2242	41.5	0.1796
	Ghosh [27]	53.0	0.3700	45.0	0.2430	41.0	0.1850
$\phi = 30^\circ$	Proposed Method	56.5	0.3076	47.5	0.1738	44.5	0.1229

$k_a$  = active earth pressure coefficient;  $\beta$  = angle of failure wedge (degrees).

researchers under similar conditions reveals an acceptable level of difference. Hence, it can be deduced that HSM has more potential than previous methods and is capable of determining static and seismic pressures, as well as the angle of failure wedge, for retaining walls under general conditions.

## REFERENCES

- Hosseini, S.M., Haeri, S.M. and Toll, D.G. "Behavior of gravely sand using critical state concepts", *Scientia Iranica*, **12**(2), pp. 167-177 (2005).
- Gholami, M. and Eslami, A. "Analytical Model for

- the ultimate bearing capacity of foundations from cone resistance”, *Scientia Iranica*, **13**(3), pp. 223-233 (2006).
3. Shahir, H. and Pak, A. “Numerical investigation of the effects of soil densification on the reduction of liquefaction-induced settlement of shallow foundations”, *Scientia Iranica, Transaction A*, **16**(4), pp. 331-339 (2009).
  4. Oliaei, M.N. and Pak, A. “Element free Galerkin meshless method for fully coupled analysis of consolidation process”, *Scientia Iranica, Transaction A*, **16**(1), pp. 65-77 (2009).
  5. Choudhury, D., Sitharam, T.G. and Subba Rao, K.S. “Seismic design of earth retaining structures and foundations”, *Current Science*, **87**(10), pp. 1417-1425 (2004).
  6. Nimbalkar, S. and Choudhury, D. “Effects of body waves and soil amplification on seismic earth pressures”, *J. of Earthquakes and Tsunamis*, **2**(1), pp. 33-52 (2008).
  7. Ahmadabadi, M. and Ghanbari, A. “New procedure for active earth pressure calculation in retaining walls with reinforced cohesive-frictional backfill”, *Geotextiles and Geomembranes*, **27**, pp. 456-463 (2009).
  8. Nouri, H., Fakher, A. and Jones, C.J.F.P. “Evaluating the effects of the magnitude and amplification of pseudo-static acceleration on reinforced soil slopes and walls using the limit equilibrium horizontal slices method”, *Geotextiles and Geomembranes*, **26**(3), pp. 263-278 (2008).
  9. Rankin, W.J.M. “On the mathematical theory of the stability of earthwork and masonry”, *Proc. of the Royal Society of London*, **8**, pp. 60-61 (1857).
  10. Coulomb, C.A. “Essai sur une application des regles de maximis et minimis a quelques de stratique relatifs a l’architecture”, in *Memoires de Mathematique et de Physique, Presentes a l’Academie Royale des Sciences*, **7**, pp. 343-82 (1776).
  11. Caquot, A. and Kerisel, F., *Tables for the Calculation of Passive Pressure, Active Pressure and Bearing Capacity of Foundations*, Gauthier-Villars, Paris (1948).
  12. Sokolovskii, V.V., *Statics of Granular Media*, Pergamon Press, New York (1965).
  13. Lee, I.K. and Herrington, J.R. “A theoretical study of the pressure acting on a rigid wall by sloping earth or rock fill”, *Geotechnique*, **22**(1), pp. 1-27 (1972).
  14. Hua, Z.K. and Shen, C.K. “Lateral earth pressure on retaining structure with anchor plates”, *J. of Geotechnical Eng., ASCE*, **113**(3), pp. 189-201 (1987).
  15. Okabe, S. “General theory of earth pressures”, *J. Japan Soc. Civil Eng.*, **12**(1) (1926).
  16. Mononobe, N. and Matsuo, H. “On the determination of earth pressure during earthquakes”, *Proc. of the World Engineering Congress, Tokyo*, **9**, pp. 179-87 (1929).
  17. Steedman, R.S. and Zeng, X. “The influence of phase on the calculation of pseudo-static earth pressure on a retaining wall”, *Geotechnique*, **40**, pp. 103-112 (1990).
  18. Zeng, X. and Steedman, R.S. “On the behavior of quay walls in earthquakes”, *Geotechnique*, **43**(3), pp. 417-31 (1993).
  19. Cheng, Y.M. “Seismic lateral earth pressure coefficients for C- $\phi$  soils by slip line method”, *Computers and Geotechnics*, **30**, pp. 661-670 (2003).
  20. Choudhury, D. and Nimbalkar, S. “Seismic passive resistance by pseudo-dynamic method”, *Geotechnique*, **55**(9), pp. 699-702 (2005).
  21. Choudhury, D. and Nimbalkar, S.S. “Pseudo-dynamic approach of seismic active earth pressure behind retaining wall”, *Geotechnical and Geological Eng.*, **24**(5), pp. 1103-1113 (2006).
  22. Shekarian, S., Ghanbari, A. and Farhadi, A. “New seismic parameters in the analysis of retaining walls with reinforced backfill”, *Geotextiles and Geomembranes*, **26**(4), pp. 350-356 (2008).
  23. Nimbalkar, S., Choudhury, D. and Mandal, J.N. “Seismic stability of reinforced soil-wall by pseudo-dynamic method”, *Geosynthetics Int.*, **13**(3), pp. 111-119 (2006).
  24. Ahmad, S.M. and Choudhury, D. “Pseudo-dynamic approach of seismic design for waterfront reinforced soil wall”, *Geotextiles and Geomembranes*, **26**(4), pp. 291-301 (2008).
  25. Shekarian, S. and Ghanbari, A. “A pseudo-dynamic method to analyze retaining wall with reinforced and unreinforced backfill”, *JSEE*, **10**(1), pp. 41-47 (2008).
  26. Azad, A., Yasrobi, S. and Pak, A. “Seismic active earth pressure distribution behind rigid retaining walls”, *Soil Dynamics and Earthquake Eng.*, **28**(5), pp. 365-375 (2008).
  27. Ghosh, P. “Seismic active earth pressure behind non-vertical retaining wall using pseudo-dynamic analysis”, *Canadian Geotechnical J.*, **45**(1), pp. 117-123 (2008).
  28. Shahgholi, M., Fakher, A. and Jones, C.J.F.P. “Horizontal slice method of analysis”, *Geotechnique*, **51**(10), pp. 881-885 (2001).
  29. Nouri, H., Fakher, A. and Jones, C.J.F.P. “Development of horizontal slice method for seismic stability analysis of reinforced slopes and walls”, *Geotextiles and Geomembranes*, **24**, pp. 175-187 (2006).
  30. Segrestin, P. “Design of sloped reinforced fill structure”, *Proc. of Conference on Retaining Structures*, Inst. of Civil Eng., Robinson College, Cambridge, pp. 574-584 (1992).
  31. Das, B.M., *Principles of Soil Dynamics*, PWS-Kent Publishing Co., Boston, MA. (1993).
  32. Zarrabi-Kashani, K. “Sliding of gravity retaining wall during earthquakes considering vertical accelerations and changing inclination of failure surface”, MS Thesis, Dept. of Civil Eng., MIT, Cambridge, MA (1979).

33. Choudhury, D. and Singh, S. "New approach for estimation of static and seismic active earth pressure", *Geotechnical and Geological Eng.*, **24**(1), pp. 117-127 (2006).

#### BIOGRAPHIES

**A. Ghanbari** obtained his BS in civil engineering from Isfahan University of Technology, Iran, in 1992, and an MS and PhD in geotechnical engineering and civil engineering from Amirkabir University of Technology Iran, in 1995 and 2002, respectively. Since 2004, Dr Ghanbari has been an Assistant Professor in the civil engineering department of Tarbiat Moallem Univer-

sity, Tehran, Iran. His main fields of research and professional activities include geotechnical earthquake engineering, soil structure interaction, dynamic and static design of earth dams, analytical methods in geotechnical engineering and geotechnical site investigation.

**Mojtaba Ahmadabadi** obtained his BS in civil engineering from Yasouj University, Iran, in 2004 and has since been a research student of geotechnical engineering at Tarbiat Moallem University, Tehran, Iran. Since 2010 he has been a faculty member of the Islamic Azad University in Sepidan, Iran.

Archive of SID